

SUPPLEMENTAL MATERIAL

Methods

Invasive Electrophysiology: Mice were anesthetized with 1-2% isoflurane in 95% oxygen. Trans-esophageal (TE) pacing was performed using a 1.1F octapolar catheter (Millar Instruments, Houston, TX) inserted into the esophagus to the level of the heart. Adequate catheter positioning was confirmed by TE pacing at 800 microvolts (μV). ECG channels were amplified (0.1 mV/cm) and filtered between 0.05 and 400 Hz. A computer-based data acquisition system (Emka Technologies, Falls Church, VA) was used to record a 3-lead body surface ECG, and 4 intraesophageal bipolar electrograms. TE pacing was performed using 2-msec current pulses delivered by an external stimulator (STG3008-FA, Multichannel Systems, Reutlingen, Germany).

Standard clinical EP pacing protocols were used to induce AF as previously described.¹ Briefly atrial burst pacing was performed with 300 cycles of 2 millisecond bursts at 800 mV and at a cycle length (CL) of 50 msec, 40 msec, 30 msec, 25 msec, 20 msec and 15 msec. Next, Verheule's pacing protocol was performed with 2-second burst cycles at CL of 40 msec, and then decreasing in each successive burst with a 2-msec decrement down to a CL of 20 msec.²⁰ This was followed by right atrial burst pacing with eight 50-ms and four 30-ms cycle length trains episodes repeated several times, up to a maximum 1-min time limit of total stimulation. Series of bursts was repeated twice. AF was defined as a period of rapid irregular atrial rhythm lasting at least 5 second. If 1 or more bursts in the 2 series of bursts evoked an AF episode, AF was considered to be inducible in that animal; otherwise, AF was considered to be non-inducible.

Echocardiography: Mice were anesthetized with 2% isoflurane and underwent transthoracic echocardiography using the VisualSonics Vevo 2100 Imaging System with a 30 MHz probe. B-mode short axis images and M-mode images were acquired as described.² Briefly, mouse chests were depilated using Nair crème, and mice were placed supine on a heated ECG board. Temperature was maintained between 36.5°C and 37.5°C, and heart rate was maintained above 400 beats per minute (bpm) in order to prevent complications including hypothermia and bradycardia. All measurements and calculations will be averaged from 3 consecutive cycles and performed according to the American Society of Echocardiography guidelines.³ Data analysis was performed offline with the Vevo 770 Analytic Software.

BP Measurements: BP was recorded in conscious mice using a noninvasive tail cuff BP System (CODA, Kent Scientific, Torrington, CT). Mice were placed into restraint tubes over a warming plate, and the BP tail cuff was attached. After a period of acclimation, a total of 30 cycles per animal was decided on to optimize the number of measurements. The first 10 cycles were not used in the final analysis. The remaining 20 cycles were evaluated according to the manufacturer's recommendations. BP was recorded in a proper environment (room temperature, lighting, and noise-free atmosphere) for 3 groups, with 5 animals in each group. Diastolic BP, systolic BP, and mean arterial pressures (MAP) were measured.

Serum Glucose Measurements: Animals were fasted for 12 hours (overnight) prior to the first blood glucose measurement. Mice were fixed by a retainer and the tail was snipped using sterile, sharp surgical scissors. The blood was gently milked from the tail

with the blood placed on a glucose test strip and read using a glucometer (Precision Neo, Chicago, IL).

Western Blotting: Atrial lysates were prepared from flash-frozen mouse hearts as previously described.⁴ Lysates from DIO and control mice were size-fractionated on 6% SDS-polyacrylamide gels. The resolved gels were electro-transferred on nitrocellulose membranes. Membranes were probed with anti-Nav1.5 monoclonal antibody (1:500 dilution; Alomone Labs #ASC005, Israel), anti-CaMKII delta polyclonal antibody (1:500 dilution; Proteintech #154431AP, USA), anti-Kv1.5 polyclonal antibody (1:600 dilution; Proteintech #216591AP, USA), anti-Kcnh2 polyclonal antibody (1:1000 dilution; abcam; #ab196301, USA); anti-PKC α polyclonal antibody (1:1000; abcam; # ab4124, USA), anti-PKC- δ recombinant antibody (1:1000; abcam; #ab182126), anti-Nox2/gp91phox antibody (1:1000; abcam; #ab80508), anti Kv4.2 polyclonal antibody(1:200; ; Alomone Labs; #APC023), anti-CaV1.2 polyclonal antibody (1:1000 dilution;Thermofisher #PA518891, USA) anti-Cx40 polyclonal antibody (1:1000 dilution; Thermosfisher #364900, USA), anti-Cx43 polyclonal antibody (1:500 dilution; Proteintech #26981AP, USA), anti-NCX1 polyclonal antibody (1:1000 dilution; Proteintech #550751AP, USA), anti-Vinculin monoclonal antibody (1:2000 dilution; Proteintech #663051Ig, USA), anti-Ryanodine Receptor 2 polyclonal antibody (1:1000 dilution; Chemicon International Inc. #AB9080 , USA) and anti-SERCA2 ATPase monoclonal antibody (1:1000 dilution; Thermofisher #MA3919, USA) at 4°C overnight. The gels were developed using anti-rabbit HRP (1:2500 dilution, Abcam, Cambridge, UK) and scanned on a Biorad Gel Doc (Hercules, CA). Protein signal densities were normalized to the corresponding β -actin or vinculin or GAPDH signal densities, and used for plotting data.

Immunohistochemistry: Atrial sections were embedded in paraffin and then dehydrated through a graded series of alcohol and PBS. Sections were washed once in PBS, permeabilized with 0.025% Triton X-100 for 10 minutes, and then blocked with 1% BSA in TBS for 1hr. Sections were then incubated with primary antibodies including rabbit polyclonal anti-Nav1.5 (1:100, Alomone Labs, Israel), rabbit polyclonal anti-4-HNE antibody (1:100, Abcam, USA) overnight at 4°C. After washing with TBS-0.025% Triton X-100, atrial sections were further treated with fluorescence-coupled antibodies (1:1000, Alexa488- and/or Alexa555, Life technologies, USA) for 1 hr at room temperature individually. All sections were stained with DAPI and mounted in mounting medium. Stained sections were imaged under a Zeiss laser scan confocal microscope LSM710 at 40X and 80X magnifications. The corrected total cell fluorescence (CTCF) was measured by quantifying the average integrated mean fluorescence intensity of individual cells in the sections using ImageJ.

Current Recordings in Mouse Atrial Cells: Atrial myocytes were isolated from control, and DIO mice using a simplified Langendorff-free isolation protocol for viable cardiac myocytes isolation from adult mouse hearts as described in Supplemental Methods.⁵ Patch-clamp measurements were performed in whole-cell configurations using an Axopatch 200B amplifier controlled by pClamp10 software.⁶ I_{Na} was recorded in a bath solution (in mmol/l): 5 NaCl, 1 MgCl₂, 1 CaCl₂, 0.1 CdCl₂, 10 Glucose, 130 CsCl, 20 HEPES, adjusted to pH 7.3 with CsOH. An intracellular solution contained (in mmol/l): 5 NaCl, 135 CsF, 10 EGTA, 5 MgATP, 10 HEPES, with pH adjusted to 7.2 with CsOH. Theoretically, the sodium reversal potential will be around 0 mV. Steady-state activation G-V for I_{Na} were fitted by the Boltzmann equation as described previously:⁷

$G/G_{max}=1/(1+\exp(V_{1/2}-V)/K)$, where G/G_{max} is the relative conductance normalized by the maximal conductance, $V_{1/2}$ is the potential of half activation, V is test pulse, and k is the Boltzmann coefficient. Pipettes had 2-4 M Ω access resistance. Current densities were calculated by whole-cell current amplitude and capacitance value taken from readings of the amplifier after electronic subtraction of the capacitive transients.

For I_{Ca-L} recording, the external solution contained (in mmol/l) 140 CsCl, 5.0 TEA-Cl, 2 CaCl₂, 1 MgCl₂, 10 HEPES, 5 Glucose, adjusted to pH 7.4 with methanesulfonic acid. An intracellular solution contained (in mmol/l) 135 CsCl, 1 MgCl₂, 10 EGTA, 0.1 CaCl₂, 4 Mg-ATP, 0.5 Na-GTP, 10 HEPES and adjusted to pH 7.3 with CsOH. Calcium currents were measured from a holding potential of -80 mV to test potentials ranging between -60 to +60 mV in 10 mV steps. For I_{Kur} recordings, the external solution contained (in mmol/l) 110 NaCl, 4 KCl, 1 MgCl₂, 1.8 CaCl₂, 10 HEPES, 5 glucose, adjusted to pH 7.35 with NaOH. The intracellular pipette solution contained (in mmol/L): 110 potassium aspartate, 20 KCl, 8 NaCl, 10 HEPES, 4 K₂ATP, 1 CaCl₂, 1 MgCl₂, 0.2 CdCl₂, 10 K₂BAPTA, adjusted to pH 7.2 with KOH. The potassium currents were produced by depolarization to -40 mV for 100 ms and then to +10 mV for 400ms from a holding potential of -80 mV; the currents were treated with 100 μ m 4-AP, and I_{Kur} was obtained as 4-AP sensitive current.⁸

AP Recording in Mouse Atrial Cells: Atrial myocytes were isolated from control, and DIO mice using a simplified Langendorff-free isolation protocol.⁵ Atrial cells were studied in current-clamp mode by injecting stimulus current (1-2 nA, 2 ms) at 1 Hz. APs were recorded at 37°C in Tyrodes solution containing: 140 NaCl, 5.4 KCl, 1 MgCl₂, 1.8 CaCl₂, 5.5 glucose, 10 HEPES (pH adjusted to 7.4 with NaOH). The pipette solution contained:

125 K-glutamate, 20 KCl, 10 NaCl, 5 EGTA, and 10 HEPES (pH adjusted to 7.2 with KOH).

Figure Legends

Figure 1: Expression of connexin and calcium handling proteins is unchanged in diet-induced obese (DIO) mouse model. **A:** Western blots of connexin (Cx) 43 expression in control and DIO mice (N=6 hearts each). **B:** Quantification of Cx43 expression in the 2 groups. **C:** Western blots of Cx40 expression in control and DIO mice (N=6 hearts each). **D:** Quantification of Cx40 in the 2 groups. **E:** Western blots of Kv4.2 (transient outward potassium channel; n=6 cells). **F:** Fold change in Kv4.2 expression in the 2 groups. **G:** Relative cell conductance normalized for maximal conductance (G/G_{\max}) for $I_{Ca,L}$; curves are Boltzmann fits of the data points (n=6, and 6 cells). *P<0.05; **P<0.01.

Figure 2: Expression of calcium handling proteins in DIO mouse model. **A:** Western blots of SERCA2a in control and DIO mice (N=6 hearts). **B:** Quantification of SERCA2a expression in the 2 groups of mice (N=6 hearts). **C:** Western blots of ryanodine receptor type 2 (RyR2) in control and DIO mice (N=6 hearts). **D:** Quantification of RyR2 expression in the 2 groups of mice (N=6 hearts). **E:** Western blots of calcium/calmodulin kinase II (CaMKII) delta expression in control and DIO mice. **F:** Quantification of CaMKII delta expression in the 2 groups of mice. **G:** Western blots of sodium-calcium exchanger 1 (NCX1) expression in control and DIO mice (N=6 hearts). **H:** Quantification of NCX1 expression in the 2 groups of mice (N=6 and 6 hearts). *P<0.05; **P<0.01.

Figure 3: The antioxidant MitoTEMPO (MT) reverses atrial fibrosis and reduces oxidative stress in DIO mice. **A:** Western blot showing NOX2 expression in DIO and DIO-MT mice (N=6 hearts). **B:** Quantification of reduced NOX2 expression in DIO MT

compared to DIO mice (N=6 hearts). **C**: Mitosox staining image in DIO and DIO-MT mice (N=6 hearts). **D**: Isoprostane levels in the control and DIO mice pre- and post-MT treatment (N=6 hearts). *P<0.05. **E**: Masson's trichrome staining of atrial myocytes from DIO mice before and chronic MT treatment. **F**: Fold change in fibrosis (%) in the 2 groups of mice showing a significant reduction in fibrosis after MT (n=6, 6). *P<0.05; **P<0.01.

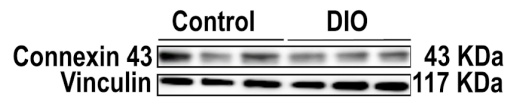
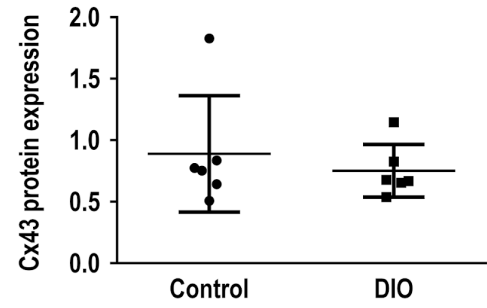
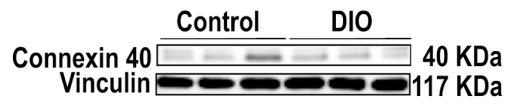
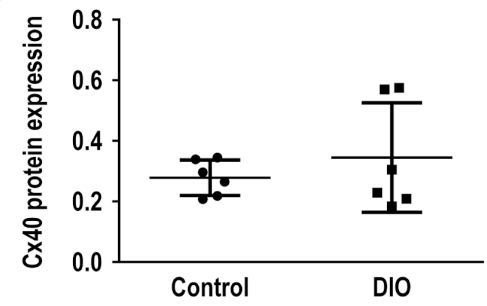
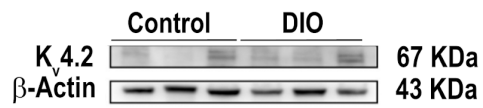
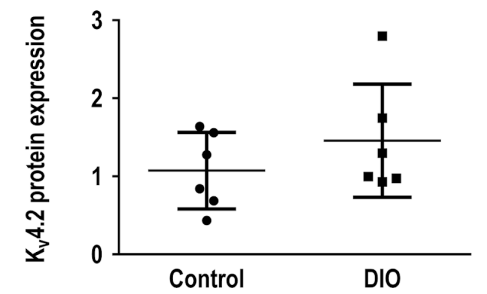
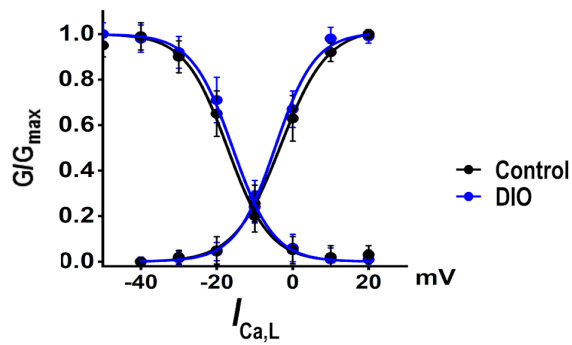
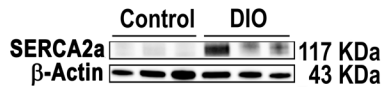
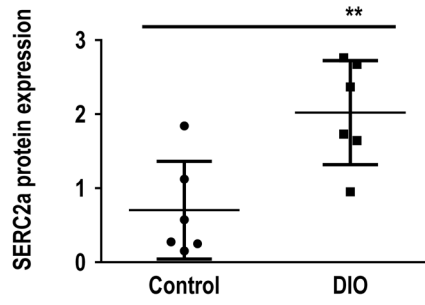
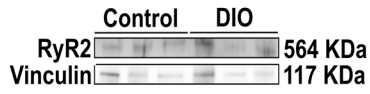
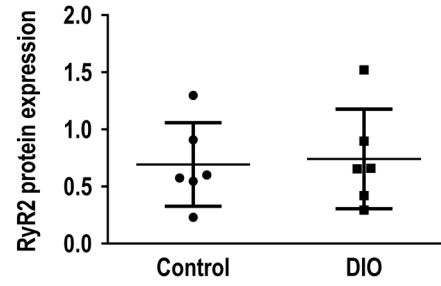
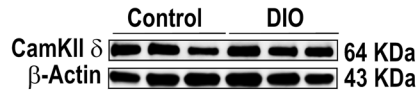
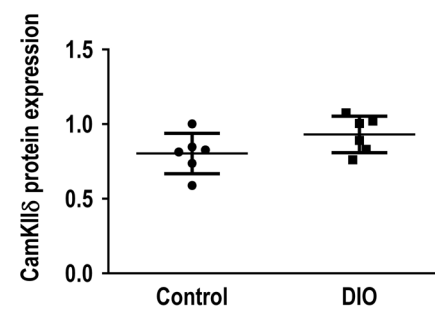
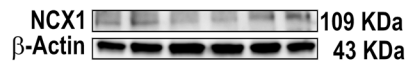
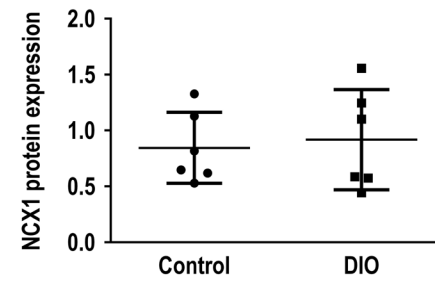
A**B****C****D****E****F****G**

Figure 1.

A**B****C****D****E****F****G****H****Figure 2.**

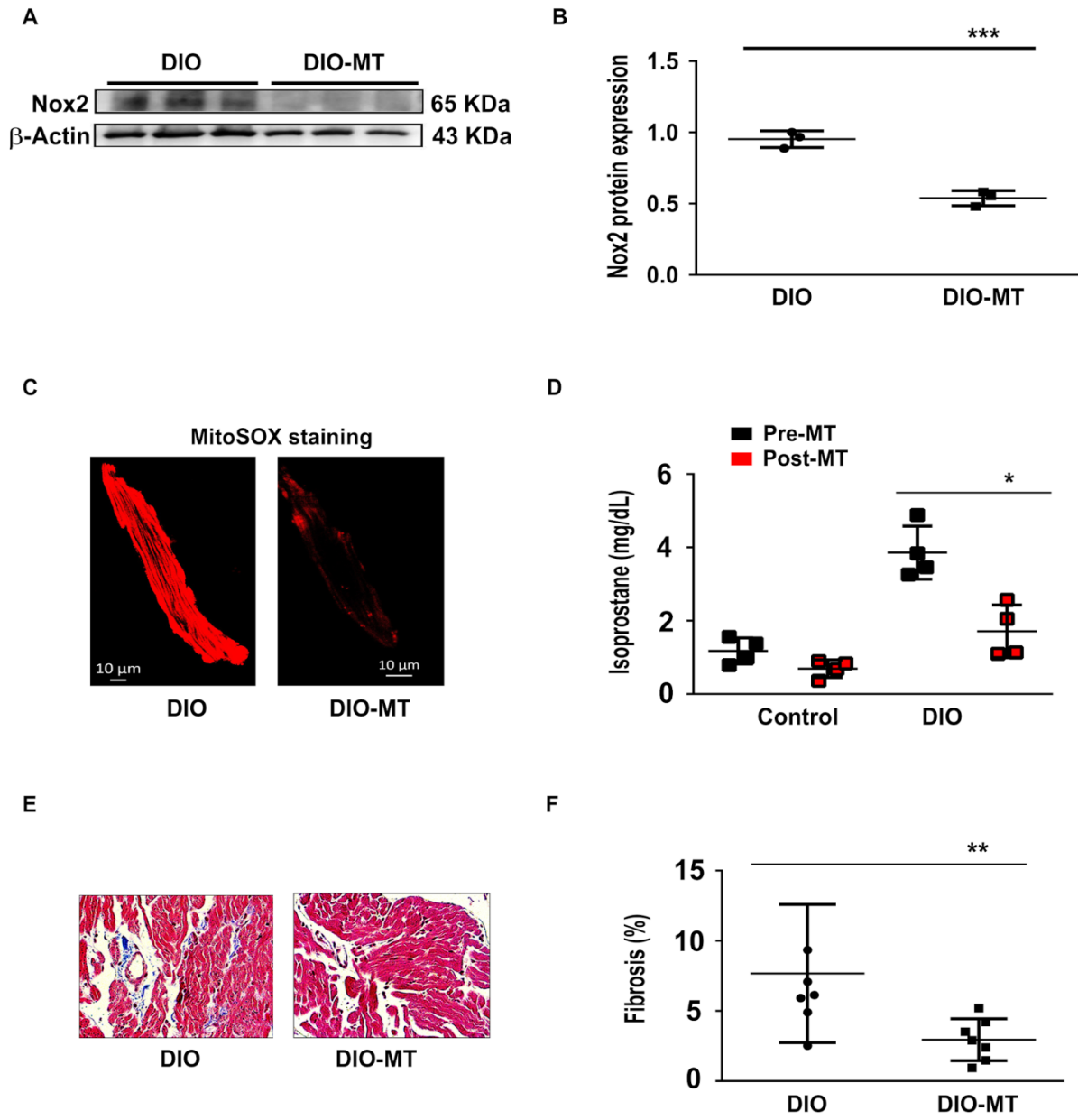


Figure 3.

References for Supplemental Methods

1. Li N, Wang T, Wang W, Cutler MJ, Wang Q, Voigt N, Rosenbaum DS, Dobrev D, Wehrens XH. Inhibition of CaMKII phosphorylation of RyR2 prevents induction of atrial fibrillation in FKBP12.6 knockout mice. *Circ Res*. 2012;110:465-70.
2. Respress JL, van Oort RJ, Li N, Rolim N, Dixit SS, deAlmeida A, Voigt N, Lawrence WS, Skapura DG, Skardal K, et al. Role of RyR2 phosphorylation at S2814 during heart failure progression. *Circ Res*. 2012;110:1474-83.
3. Nagueh SF, Smiseth OA, Appleton CP, Byrd BF, 3rd, Dokainish H, Edvardsen T, Flachskampf FA, Gillebert TC, Klein AL, Lancellotti P, et al. Recommendations for the Evaluation of Left Ventricular Diastolic Function by Echocardiography: An Update from the American Society of Echocardiography and the European Association of Cardiovascular Imaging. *European heart journal cardiovascular Imaging*. 2016;17:1321-1360.
4. van Oort RJ, McCauley MD, Dixit SS, Pereira L, Yang Y, Respress JL, Wang Q, De Almeida AC, Skapura DG, Anderson ME, et al. Ryanodine receptor phosphorylation by calcium/calmodulin-dependent protein kinase II promotes life-threatening ventricular arrhythmias in mice with heart failure. *Circulation*. 2010;122:2669-79.
5. Ackers-Johnson M, Li PY, Holmes AP, O'Brien SM, Pavlovic D, Foo RS. A Simplified, Langendorff-Free Method for Concomitant Isolation of Viable Cardiac Myocytes and Nonmyocytes From the Adult Mouse Heart. *Circ Res*. 2016;119:909-20.
6. Kim IH, Hevezi P, Varga C, Pathak MM, Hong L, Ta D, Tran CT, Zlotnik A, Soltesz I, Tombola F. Evidence for functional diversity between the voltage-gated proton channel Hv1 and its closest related protein HVRP1. *PLoS One*. 2014;9:e105926.

7. Pathak MM, Tran T, Hong L, Joos B, Morris CE, Tombola F. The Hv1 proton channel responds to mechanical stimuli. *J Gen Physiol.* 2016;148:405-418.
8. Schumacher-Bass SM, Vesely ED, Zhang L, Ryland KE, McEwen DP, Chan PJ, Frasier CR, McIntyre JC, Shaw RM, Martens JR. Role for myosin-V motor proteins in the selective delivery of Kv channel isoforms to the membrane surface of cardiac myocytes. *Circ Res.* 2014;114:982-92.